New Concept Fuel Characterization by Micro Flow Reactor with Controlled Temperature Profile

Kaoru Maruta, Hisashi Nakamura, Takuya Tezuka and Susumu Hasegawa
Energy Dynamics Laboratory, TFI, IFS, Tohoku University

An original methodology for fuel characterization, a micro flow reactor with a controlled temperature profile was applied for Primary Reference Fuel of gasoline (blended fuel of n-heptane and iso-octane, PRF). Combustion and ignition characteristics of a stoichiometric gaseous PRF/air mixture were investigated.

By changing the mixture flow velocity at the inlet of the reactor, three kinds of flames were observed: normal propagating flame in a high flow velocity region; unstable flames, named flames with repetitive extinction and ignition (FREI), in an intermediate flow velocity region; and stable multiple weak flames in a low flow velocity region. In the weak flame phenomenon, multi-stage oxidation process of the fuel in a wide temperature range from 600-1200 K can be observed as separated multiple stationary flames. Focusing on this low flow velocity condition, weak flame responses to octane number under atmospheric pressure were examined using PRFs with various octane numbers. As octane number increased, luminosity from low temperature oxidation was decreased and the main reaction shifted to the high temperature region. The capability of the present reactor for examination of the general ignition characteristics of various fuels was demonstrated.

In addition, pressure dependence of the weak flames was investigated using PRFs with various octane numbers. Low temperature oxidation exhibited more significant heat release under elevated pressure, and this change was dependent on the octane number.

To examine the experimental results, one-dimensional steady computation was conducted using detailed reaction kinetics. Computational results reproduced the tendencies of the experimental results qualitatively.

Both the experimental and computational results indicate the advantage of the separate investigation of the oxidation process in each temperature region, which can be realized only by the present micro flow reactor, to obtain a detailed understanding of the ignition characteristics of practical fuels.

6.1. Introduction

6.1.A. Motivation

It is urgently required to develop technologies to control internal combustion devices more efficiently in terms of energy savings. Especially for improving the efficiency of compression ignition engines, the understanding of the ignition process of various fuels would play an important role.

This study focused on ignition characteristics of a blended fuel of n-heptane and iso-octane. The blended fuel of n-heptane and iso-octane is used as the simplest Primary Reference Fuel (PRF), which represents the combustion characteristics of gasoline. In addition, the mixing ratio of n-heptane and iso-octane corresponds to Research Octane Number (RON), which is an index of anti-knock ability.

The ignition process of PRF/air has been investigated mainly by using rapid compression machines (RCMs). Time-histories of pressure and species in the RCM chamber are measured. Reaction kinetics models are validated by comparing the predicted ignition delay times and concentration time-histories of reactants, intermediates, and products with the experimental results [1-3]. Ignition delay times of two-stage ignition [4] and concentration time-history of formaldehyde, which is a typical product of kinetic processes associated with cool flame [1], have also been investigated.

As a weak point of RCMs, however, difficulty of accurate tracking of the gas-phase temperature history in the chamber should be mentioned. Sources of errors cannot be fully eliminated due to, e.g., heat loss through the wall during auto-ignition and temperature non-uniformity in the combustion chamber.

Therefore, a well defined, simple experimental system for investigation of the ignition process is required. For that reason, this study focused on a micro flow reactor with a controlled temperature profile [5, 6] as an alternative experimental method.

6.1.B. Micro flow reactor with a controlled temperature profile

In the context of fundamental studies on microcombustion [7-9], combustion in a heated channel with an inner diameter smaller than the ordinary quenching diameter for room temperature condition was conducted [5, 6]. Some studies were conducted with the similar configuration [10-13]. Recently, it is recognized that such configuration can be utilized as micro flow reactor with temperature gradient for examining ignition and combustion characteristics of given fuels [14-17].

In the micro flow reactor, quartz glass tube with an inner diameter smaller than the ordinary quenching diameter for room temperature condition is heated by an external heat source so as to have a stationary temperature profile along the inner surface of the tube in the axial direction. A fuel/air mixture flows into the tube, and then a flame is formed.

Due to the small inner diameter, the temperature of the gas phase in the tube strongly depends on the temperature of the inside surface of the tube. Flow in the tube is laminar and pressure in the tube is constant. Effect of surface reaction on the flame behavior was confirmed to be negligible in our previous study [16].

In previous studies using this micro flow reactor, Tsuboi et al. found that there is a lower inlet flow velocity limit of methane/air weak flame and that wall temperature at the flame position corresponds to the minimum ignition temperature of the fuel in a given condition [14, 15]. Oshibe et al. observed weak flames of DME/air in the micro flow reactor and found stabilized multi-stage oxidation including low temperature oxidation [16]. Yamamoto et al. have conducted an investigation on the multi-stage oxidation process of n-heptane/air, which consists of cool and separated hot flames [17]. These studies have clearly indicated the capability of the micro flow reactor as a method to investigate general ignition characteristics of fuels. Application of PRF as a fuel to the micro flow reactor to examine the capability of the reactor for the clarification of ignition characteristics of practical fuels is also considered to be valuable.

This study focused on the investigation of combustion and ignition characteristics of gaseous blended fuel of iso-octane and n-heptane (PRF) by using a micro flow reactor with a controlled temperature profile. The weak flame response to the various RONs was investigated by varying the mixing ratio of n-heptane and iso-octane. The pressure dependences of the weak flame were also investigated using PRF/air with various RONs.

In addition, one-dimensional computations were conducted using a detailed reaction mechanism [18, 19] of PRF. Obtained computational results were compared with experimental results.

6.2. Experimental and Computational methods

6.2.A. Experimental method

A schematic of the experimental setup is shown in Fig. 6.1. A quartz glass tube was heated by a H_2/air premixed burner so as to have a stationary temperature profile (300-1300 K) along the inner surface of the tube in the axial direction. H_2/air burner was chosen as an external heat source for better visualization of chemiluminescence from hydrocarbon flames in the micro flow reactor. The maximum wall temperature and temperature profile can be adjusted by changing the equivalence ratio, the flow velocity of an H_2/air mixture, and the distance between the tube and the burner.

For experiments under atmospheric pressure, a quartz glass tube with an inner diameter of 2 mm was employed. A gaseous premixture of PRF/air was produced by injecting liquid PRF with a micro-syringe (Hamilton: 1700 series) into heated air. Air temperature at the upstream side of the injection position was controlled to be 300-323 K by an electric heater to assure vaporization. The flow rate of air was controlled by a mass flow controller and the injection volume of liquid PRF was controlled by a mechanical stage with a stepping motor to maintain the equivalence ratio as unity. n-Heptane and iso-octane were blended in

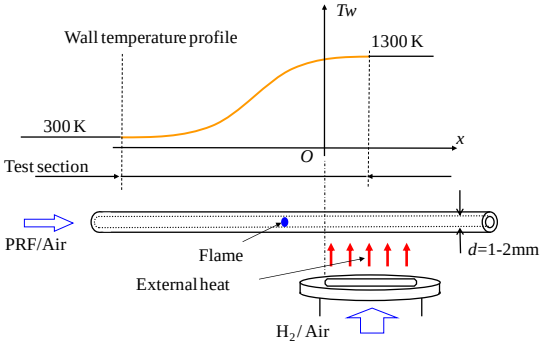

Fig. 6.1. Experimental setup.

the required ratio in the liquid state beforehand. Purities of both n-heptane and iso-octane are higher than 99 % (Wako Pure Chemical Industries).

In the elevated pressure experiments, a quartz glass tube with an inner diameter of 1 mm was used. This is because the quenching diameter becomes smaller under elevated pressure. In addition, a different mixture supplying method was employed because of difficulties of using the syringe for elevated pressure setups. A gaseous PRF/N_2 mixture was stored in a tank at 6 atm and 373 K in advance. A gaseous premixture of PRF/air was then produced by mixing PRF/N_2 and O_2. Flow rates of the PRF/N_2 mixture and O_2 were controlled by each mass flow controller and a stoichiometric gaseous PRF/N_2/O_2 mixture was fed into the tube. The ratio of N_2 to O_2 was the same as that of an air. Pressure in the tube was controlled by a pressure regulator installed at downstream of the flow reactor, and it was changed from 1 to 5 atm in this study.

A gaseous PRF/air mixture flowing into the quartz tube ignites at the high temperature region and flame is formed at a certain position. Images of this flame were captured with a digital still camera (Nikon D200 or D300). The cameras were equipped with optical band-pass filters (transparent wavelength: 431.4 nm, half bandwidth: 6.4nm) for better observation of chemiluminecsence from hydrocarbon flames by eliminating thermal radiation from the heated tube.

Flame location was defined at the peak of the luminosity distribution which was obtained from the captured flame image. The upstream side edge of the H_2/air burner was defined as x = 0.

After capturing the flame images, wall temperature measurement was conducted under atmospheric pressure with a K-type thermocouple (diameter of 50 μm) inserted from the exit of the tube. Flow velocity was maintained the same as the experimental condition by flowing air flow. Changes of the wall temperature profile due to the pressure increase were confirmed to be negligible because the heat capacity of the tube wall is much larger than the increased heat capacity of the gas phase even under the elevated pressure.

6.2.B. Computational method

To further examine the experimental results, one-dimensional steady computations were conducted with a code based on PREMIX [20], which models a reactive flow in the micro flow reactor. Heat convection term between the gas phase and the wall was added to the energy equation [5] as follows:

$$\dot{M}\frac{dT}{dx}-\frac{1}{c_p}\frac{d}{dx}\left(\lambda A\frac{dT}{dx}\right)+\frac{A}{c_p}\sum_{k=1}^{K}\rho Y_k V_k c_{pk}\frac{dT}{dx}+\frac{A}{c_p}\sum_{k=1}^{K}\dot{\omega}_k h_k W_k-\frac{A}{c_p}\frac{4\lambda Nu}{d^2}(T_w-T_g)=0$$

In the heat convection term, the wall temperature profile from 300 to 1300 K, which is the same as the experimental condition, was given as Tw. The Nusselt number was selected to be constant (Nu = 4) based on the facts that it is 4.36 for a constant heat flux and 3.66 for constant wall temperature for a steady, fully developed laminar flow of a constant density fluid. Although a specific Nusselt number in such a combustion field with solid theoretical basis cannot be found, it was confirmed that the positions of weak flames were insensitive to the Nusselt number.

Detailed reaction mechanism of PRF developed by Curran et al. (1034 species, 4236 reactions) [18, 19] was selected. The computational region was 10 cm long and the equivalence ratio was unity, the same as that in the experimental condition. Transport model provided at LLNL website [18, 19] was used. Thermal diffusive effect was considered and micture-avaraged model was adopted. Flame location was defined as the peak of heat release rate (HRR) profile.

6.3. Results and discussion

6.3.A. iso-Octane/air flame responses to various inlet flow velocities.

Flame responses to the mixture flow velocity at the tube inlet were investigated using a PRF100 (iso-octane 100%)/air mixture under atmospheric pressure. Figure 6.2 shows the flame location in relation to various inlet flow velocities. The horizontal axis of Fig. 6.2 is the location along the tube and the origin of x-axis was set at the upstream edge of the H_2/air burner. The vertical axis in Fig. 6.2 is the mixture flow velocity. Figure 6.3 shows the images of the flames captured in each flow velocity condition. The flow direction is from left to right in the figure. As shown in the figures, three kinds of flame response were observed with changing mixture flow velocity.

Stable flame (Normal flame) was observed in a high flow velocity region (U > 50 cm/sec). Unstable flames called flames with repetitive extinction and ignition (FREI) [5] were observed in an intermediate flow velocity region (U = 8-50 cm/s). Stable flames with weak luminescence (Weak flames) were observed in a lower flow velocity region (U < 8 cm/sec). This tendency, that is, the existence of three kinds of flame response observed by changing the mixture flow velocity, agrees with the previous experimental results for methane [14, 15], DME [16], and n-heptane [17], and theoretical analysis (described in the section 3.1.2.) by Minaev et al. [21]. Details of the each flame are described in the following sections.

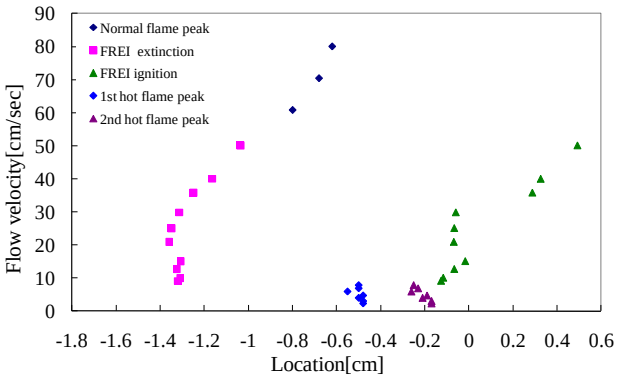

Fig. 6.2. Location of captured flames with various mean flow

6.3.A.1. Normal flame and FREI observed in high and intermediate flow velocity regions

In the high flow velocity region (U > 50 cm/sec), ordinary planar propagation flame (Normal flame) was observed. Positions of the captured flame are plotted in Fig. 6.2. With the decrease of the mixture flow velocity, the flame position shifted to the upstream side.

In the intermediate flow velocity region (U = 8 - 50 cm/sec), unstable oscillatory flames, termed FREI [5], were observed. Figure 6.4 shows the FREI images captured with the high speed video camera. The incoming mixture flowing into the hot downstream region ignites at a certain location and the ignition kernel propagates to the upstream side. However, it is quenched at a certain location in the upstream region due to the larger heat loss to the low temperature wall. After some time delay, a fresh incoming mixture ignites in the high temperature region again and this cycle is repeated rapidly. That is why FREI shows a thick flame zone, as shown in Fig. 6.3(b), when its image is captured by the digital still camera.

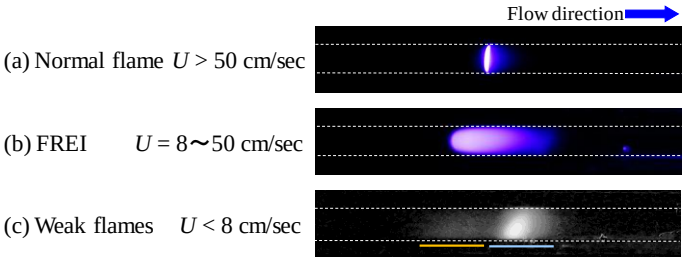

Fig. 6.3. Flame images captured through optical filter: (a) Normal flame (U = 51 cm/s),(b) FREI (U = 10 cm/s), and (c) Weak flames (U = 1.6 cm/s).

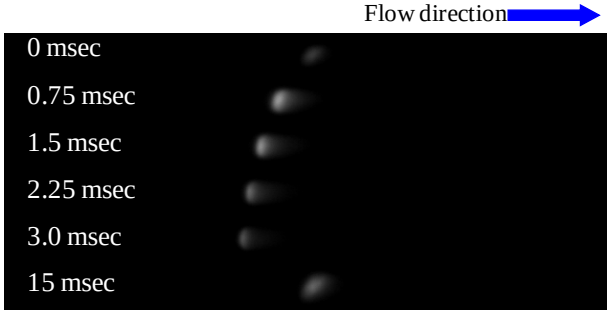

Fig. 6.4. FREI images captured with high speed Camera and image intensifier.

For that reason, the obvious flame location of FREI can hardly be defined from Fig. 6.3(b). Therefore, the ignition position was defined where normalized luminosity reached 20%, and the extinction position was where it fell below 20% in the Fig. 6.2. Detailed description of the FREI phenomenon and its analytical description can be found elsewhere [5, 21], and similar flame dynamics have also been reported in some studies on microcombustion [10, 12, 13, 22].

6.3.A.2. Weak flames observed in low flow velocity region

Stable weak flames as shown in Fig. 6.3(c) were observed in the low flow velocity region. These weak flames were captured with long exposure time (30-180 sec), since weak flames have very weak luminosity. Background subtraction was done for Fig. 6.3(c), to remove the luminosity of thermal radiation from the heated tube. With long exposure capturing, two luminous zones were observed in the flow direction in this low flow velocity region. These luminous zones are confirmed to be separated hot flames, which have already been realized in a previous study on

weak flames of DME/air [16] and n-heptane/air [17] (details are described in section 6.3.B.2). The reaction zone which located at the upstream side, the first hot flame, has relatively milder luminosity than that at downstream side, the second hot flame.

In this low flow velocity region, weak flames are stabilized after ignition and the second hot flame position is very close to the ignition position of the FREI regime in lower flow velocity. This is because weak flames do not release enough heat to propagate like FREI. Luminous zones of both the distinct weak flames in the flow direction are broader than those of normal stable flames observed in the high flow velocity region. This is because the reaction zones are broadened in the low flow velocity region due to the significant effect of mass diffusion [14]. Note that effects of local temperature and mass diffusion dissipation rather than flow velocity are dominant in the weak flames regime [15].

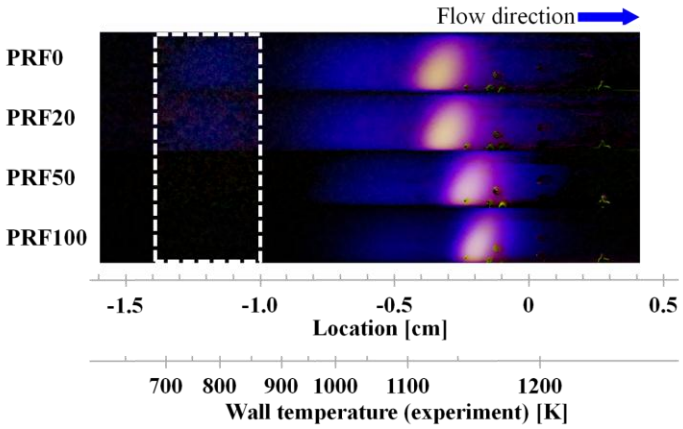

Fig. 6.5. Weak flame images of fuels with various RONs.

Theoretical analysis, which was conducted previously [Fig. 6.7 in Ref.21], shows the flame locations on S-shaped curve which has three branches. The stable branch in high flow velocity region corresponds to normal flame. And the intermediate flow velocity branch is unstable solution, where FREI phenomena were observed. An extraordinary low-velocity stable branch is weak flame. Ignition points of FREI are connected to the weak flame branch. Those points and weak flame branch cab be regarded as the conventional ignition branch in the Fendell curve. This indicates that ignition phenomena which normally observed as transient phenomena were suppressed and chemical reaction analogous to initial ignition is reproduced as steady solution in the form of "weak flames."

Change of wall temperature due to the heat release of weak flames was experimentally confirmed to be negligible. For that reason, the advantage of the micro flow reactor, that the gas-phase temperature strongly depends on solid-phase temperature, is also valid, especially in this low flow velocity condition. We can observe the ignition process under the controlled temperature and avoid complicated factors such as heat loss and roll-up vortices which make the phenomenon in RCM complicated. Observation of weak flames is expected to be efficient for investigation of the ignition process of the fuel in each temperature region. Thus, special attention will be paid to the low flow velocity region from the next section and detailed characteristics of weak flames for fuels with various RONs and various pressure levels are presented.

6.3.B. Weak flame responses to various RONs under the atmospheric pressure

This section focuses on the response of weak flames to fuels with various RONs under atmospheric pressure. Flame responses were observed by changing the mixing ratio of iso-octane and n-heptane. The inlet flow velocity was set to be 1.2 cm/sec, and PRF0, 20, 50, 100 were used as fuel.

6.3.B.1. Experimentally observed weak flame responses to various RONs

Figure 6.5 shows the images of weak flames of fuels with various RONs. Exposure time was set to be 180 sec. Background subtraction was done for the images, the same as that for Fig. 6.3 (c). In addition, luminosity level from low temperature region (enclosed by white line) is especially intensified for the comparison between fuels.

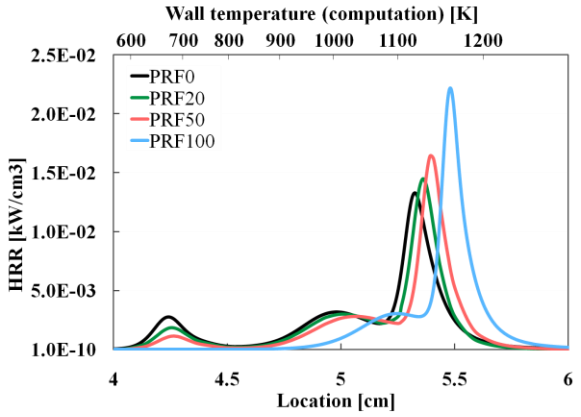

Fig. 6.6. Computed HRR and given wall temperature profile.

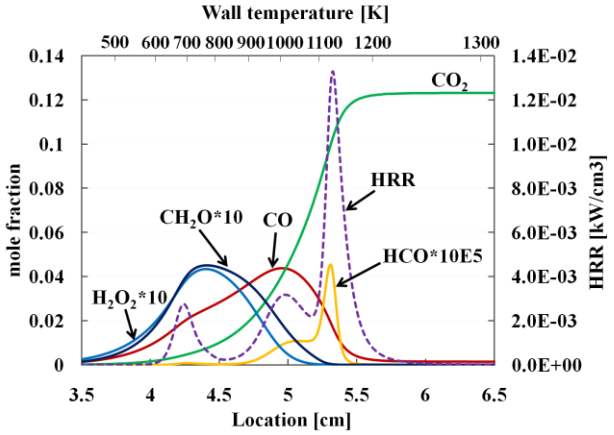

Fig. 6.7. Heat release rate and mole fractions of representative species for PRF0/air weak flames. (U = 1.2 cm/sec, P = 1 atm).

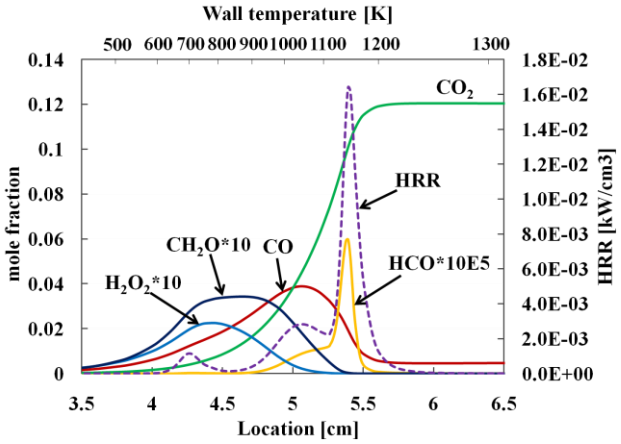

Fig. 6.8. Heat release rate and mole fractions of representative species for PRF50/air weak flames. (U = 1.2 cm/sec, P = 1 atm).

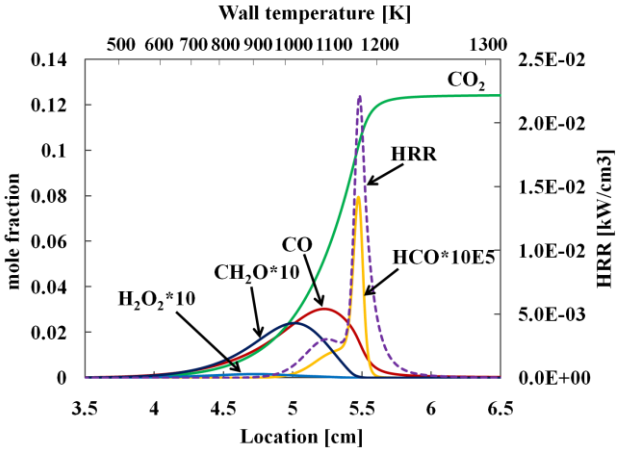

Fig. 6.9. Heat release rate and mole fractions of representative species for PRF100/air weak flames. (U = 1.2 cm/sec, P = 1 atm).

In the case of PRF0 (n-heptane 100%), two luminous zones in the downstream side (high temperature region), which are the same as in the case of iso-octane, and an additional weak luminous zone in the low temperature region were observed. This three-stage oxidation process of n-heptane was also observed by Yamamoto et al. [17]. According to the species concentration measurements in their study, the weak luminous zone in the low temperature region is confirmed to be cool flame, and the broad luminous zone in the intermediate temperature region and the brightest reaction zone in the high temperature region are separated hot flames. Reaction process of such multiple reaction zones for n-heptane was clarified in [17] and also will be discussed in 6.3.B.2. Only a weak luminosity of the cool flame was observed in the case of PRF20, but cool flame was not recognized in the case of PRF50 and PRF100. These findings show that luminosity of cool flame decreases as RON increases. In addition, it was observed that the second hot flame position shifts to the high temperature region as RON increases. The wall temperatures at the hot flame locations were 1131 K in the case of PRF0, 1159 K for the PRF50, and 1168 K for the PRF100.

6.3.B.2. Computed weak flame responses to various RONs

1-D computation was conducted to investigate the weak flame responses to various RONs under atmospheric pressure. Figure 6.6 shows the computed HRR profiles of PRF0, 20, 50, and 100, and the given wall temperature profile. Flow velocity was set to be 1.2 cm/sec and equivalence ratio was unity, the same as in the experimental condition.

In the case of PRF0, three peaks of the HRR profile were confirmed at x = 4.25, 4.98 and 5.33 cm. By conducting the gas sampling analysis [17], it has already been confirmed that these three reactions correspond to the three luminous zones observed in the case of PRF0/air in Fig. 6.5. Therefore, the peak at x = 4.25 cm is a cool flame, and peaks at x = 4.98, 5.33 cm are separated hot flames.

Table 6.1
Comparisons of wall temperatures at each flame under given conditions in unit K (U = 1.2 cm/sec, d = 2.0 mm, P = 1.0 atm, φ = 1.0).

	Fuel	PRF0	PRF50	PRF100
Experiment	cool flame	775	-	-
	1st hot flame	1031	1062	1074
	2nd hot flame	1131	1159	1168
Computation	cool flame	679	687	-
	1st hot flame	1012	1039	1105
	2nd hot flame	1127	1160	1170

On the other hand, the peak value of cool flame decreases as RON increases, and the peak of cool flame in the case of PRF100 was not confirmed. In addition, the second hot flame position shifts to the high temperature region as RON increases. These tendencies well agree with those of experimental results shown in Fig. 6.5.

Figure 6.7-9 show a HRR (dotted line) and mole fractions of major species for PRF0, 50, and 100. Computational conditions are the same as those of Fig. 6.5.

According to the case of PRF0/air, which was discussed in [17], one of the major intermediates, CO mole fraction starts increasing at the first HRR peak. It then continues increasing to the second HRR peak, and is finally consumed at the third HRR peak. CH_2O is a product of the reaction at the first HRR peak and is later consumed at the second HRR peak. H_2O_2 mole fraction shows a trend similar to that of CH_2O. The increases and decreases of species concentration at each HRR peak in the computation showed a good agreement with experimental results [17]. In typical transient multi-stage ignition, low temperature reaction, or cool flame, is characterized by the formation of CH_2O and H_2O_2 [23, 24]. These species were then consumed in the early stage of high-temperature reaction, which is called blue flame in some studies [25–27], and the large amount of CO is formed in the reaction [27, 28]. Finally, CO and other unburned species are completely oxidized to CO_2 and H_2O [28], and this reaction is called hot flame. Therefore, it is clear that the first, second and third flames in the present micro flow reactor correspond to typical cool, separated hot (or blue and hot) flames as was confirmed by species measurement in [17].

On the other hand, PRF50 and 100 show species profile of CO and HCO only qualitatively similar to that of PRF0. However, produced amount of H_2O_2 and CH_2O, the representative products of cool flame, are not as much as the case of PRF0. Especially for the case of PRF100, production of H_2O_2 is hardly observed. CO and CH_2O, which are produced gradually from low temperature for the case of PRF0, start reacting behind the 1st hot flame for the case of PRF100. These tendencies are considered to concern with very low heat release from cool flame for PRF100/air.

6.3.B.3. Comparison of experimental and computational results

Experimental and computed wall temperatures at each flame position are compared in Table 6.1. The table shows that overall tendency of each flame depending on RON was well reproduced by computation.

In regard to 2nd hot flame position, both results show that PRF0 and PRF100 differ by about 40 K. For every fuel case, the maximum difference between computed and experimental results is only a few K. That means the present 1-D modeling successfully reproduced the 2nd hot flame. In the case of cool flame, there is about 100 K difference between experimental and computed results. On the other hand, 1st hot flame shows the maximum difference of about 30 K, however, it should be noted that 1st hot flame showed the broad reaction zone.

By conducting the experiments and computations to investigate the response of weak flames to RONs, the capability of the micro flow reactor was demonstrated to distinguish and examine the difference of ignition process of fuels with various RONs since it enables separate investigation of the ignition process in each temperature region. This difference of ignition process in each temperature region for various fuels can be visualized only in the present micro flow reactor, and these results should be useful in diverse ways, for example, for analysis of reaction path, and development and validation of reaction kinetics.

In the next section, weak flame responses to various pressures using PRF0, 50, and 100 are examined, which has a significant meaning for obtaining a fundamental understanding of ignition characteristics under high pressure conditions.

6.3. C. Weak flame responses to various RONs under elevated pressures

Weak flames of PRF0 (n-heptane), PRF50, PRF100 (iso-octane) under elevated pressures were investigated to examine the pressure dependence of their ignition characteristics. Pressure range was from 1 to 5 atm.

In the experiment, flow velocity was set to be 2 cm/sec since it is hard to observe the luminosity from cool flame under the flow velocity of 1 cm/sec due to very low inflow of fuel mass. On the other hand, it was set to be 1 cm/sec in the computation because it is hard to get a converged solution under the flow velocity of 2 cm/sec and 5 atm in the computation, since it is close to the boundary with the unstable flame (FREI) regime. For that reason, experimental/computational results under different flow velocities are being compared, however, it is considered to be reasonable for showing capability of the present method based on the fact that weak flame location is not sensitive to the inlet flow velocity in such extremely low velocity region.

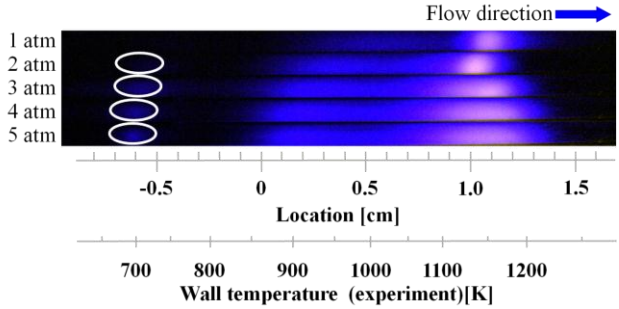

Fig. 6.10. Images of PRF0/air weak flames under elevated pressures.

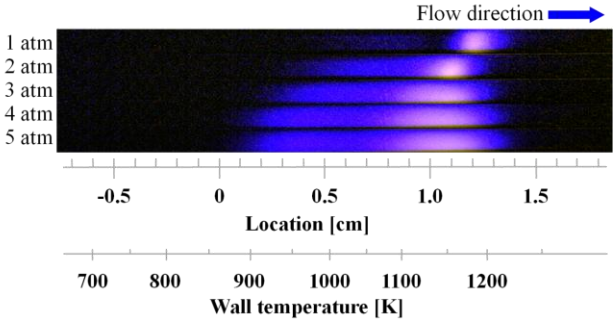

Fig. 6.11. Images of PRF100/air weak flames under elevated pressures.

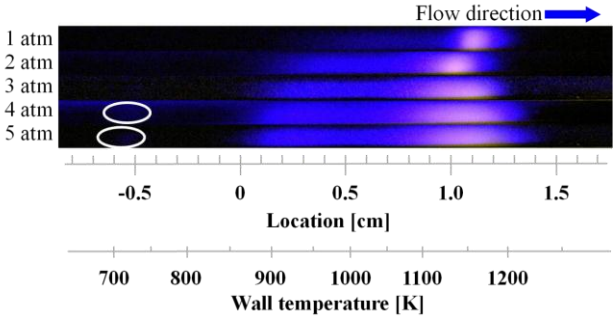

Fig. 6.12. Images of PRF50/air weak flames under elevated pressures.

6.3.C.1. Experimentally observed pressure dependence of PRF/air weak flames

Figures 6.10, 6.11 and 6.12 show the experimentally observed images of weak flames for PRF0 (n-heptane)/air, PRF100 (iso-octane)/air, and PRF50/air respectively, under atmospheric and elevated pressures (P = 1-5 atm). The flow velocity was set to be constant (U = 2.0 cm/sec). Exposure time was 180 sec and background subtraction was done for each image.

At P = 1 atm in Fig. 6.10, cool flame is not clearly observed due to very weak chemiluminescence. Hot flames are not clearly separated at P = 1 atm in Figs. 6.10-12. It should be noted that weak flame images under atmospheric pressure in Figs. 6.10-12 have different appearances from those in Fig. 6.5, which is due to the different inner diameter of the quartz tube. The wall temperature at each weak flame does not change significantly in both experimental conditions.

In the case of PRF0/air, with the increase of pressure, cool flame appeared and the first hot flame was also intensified, which led to a clear separation of hot flames. As a result, three-stage oxidation was clearly confirmed under the higher pressures. With an increase of pressure up to 5 atm, the second hot flame appeared to be broadened and the cool and first hot flames became stronger. In addition, the position of the first hot flame shifted to the upstream side with the increase of pressure. On the other hand, the second hot flame shifted to the upstream side from P = 1 to 2 atm, but tendency is reversed from P = 2 to 5 atm.

In the case of PRF100/air, cool flame was not captured even under P = 5 atm. The first and second hot flames exhibited almost the same tendency as the case of PRF0/air, i.e., as pressure increased, the first hot flame shifted to the upstream side and its luminosity became stronger, and the second hot flame shifted to the upstream side from P = 1 to 3 atm, and the tendency is reversed at higher pressures.

In the case of PRF50/air, very weak chemiluminescence of the cool flame was visible only in the cases of P = 4-5 atm. Including the first and second hot flames, the response of weak flames to a pressure change for PRF50 had intermediate characteristics between those of PRF0/air and PRF100/air.

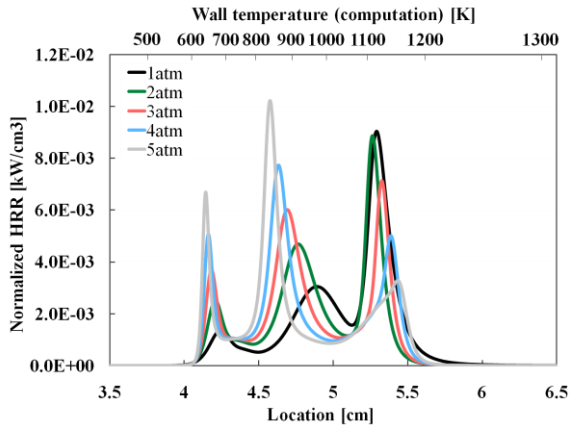

Fig. 6.13. Normalized computed HRR of PRF0/air weak flames under elevated pressures.

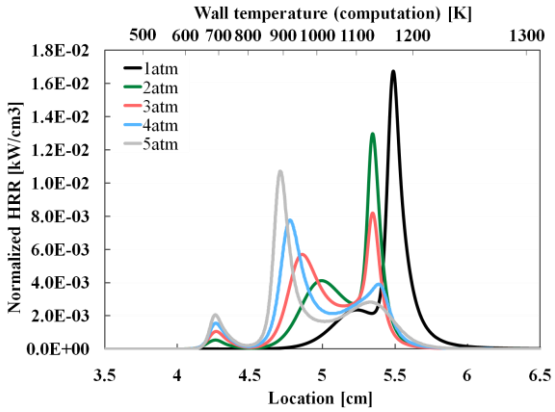

Fig. 6.14. Normalized computed HRR of PRF100/air weak flames under elevated pressures.

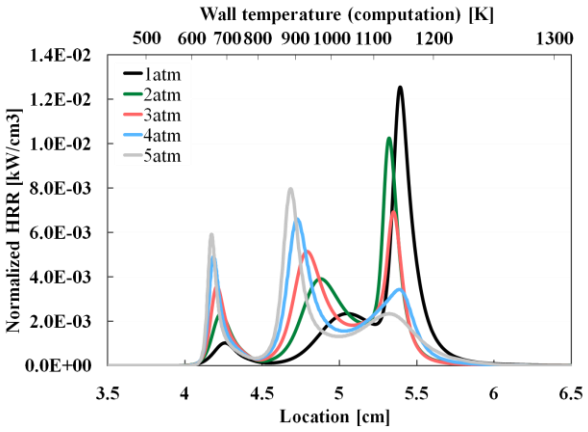

Fig. 6.15. Normalized computed HRR of PRF50/air weak flames under elevated pressures.

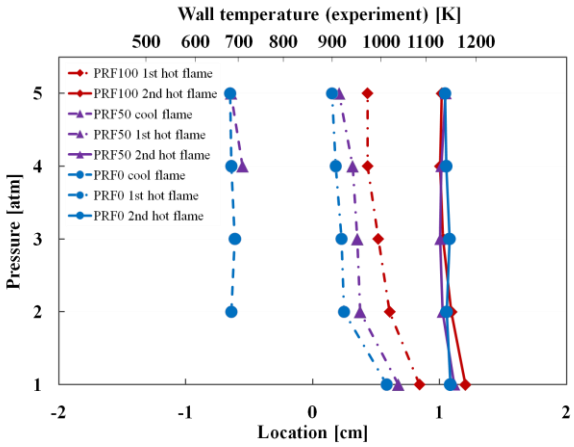

Fig. 6.16. Experimentally confirmed weak flame position to pressure

6.3.C.2. Computed pressure dependency of the weak flames

Figures 6.13, 6.14, and 6.15 show the computed HRR profile of weak flames of PRF0/air, PRF100/air, and PRF50/air, respectively, under pressure from 1 to 5 atm. The flow velocity was set to be 1.0 cm/sec. For the case of elevated pressures, the amount of total heat release was normalized (HRR was simply divided by the value of pressure) to equalize to that of the atmospheric pressure in these figures.

In Fig. 6.13, there are three HRR peaks in the flow direction, and the HRR peak of the second hot flame is strongest under atmospheric pressure. As pressure increases, intensities of the HRR peaks of the cool flame and the first hot flames become stronger and that of the second hot flame is relatively weakened. In addition, while the cool and first hot flames shift to the upstream side with increasing pressure, the second hot flame shifts to the upstream side from P = 1 to 2 atm, then shifts to the downstream side from P = 2 to 5 atm.

In the case of PRF100/air, the HRR peak of the cool flame was obtained only under elevated pressures. However, the peak value was much smaller than that of PRF0/air. On the other hand, the first and second hot flames showed pressure dependence similar to that of PRF0/air. The second hot flame shifted most upstream under P = 3 atm.

In the case of PRF50/air, the HRR peak of the cool flame increased as pressure increased. However, it was not so significant as the case of PRF0/air. On the other hand, the first and second hot flames both showed tendencies similar to those of the cases of PRF100/air and PRF0/air. Overall tendencies of HRR are intermediate between those of PRF0 and PRF100.

6.3.C.3. Comparison of the experimental and computational results

By comparing the computational results with experimental results, qualitative tendencies of each weak flame's behavior are in good agreement with each other. Figures 6.16 and 6.17 show the positions of each flame obtained from the experiments and computations, respectively. Table 6.2 shows the comparison of experimental and computational wall temperatures at each flame under the pressure of 5 atm. The experimental and computational results both show that there is only a small pressure dependence of the position of the second hot flame. However, it is difficult to confirm the position of the second hot flame due to its broadening chemiluminescence under the elevated pressure. The shift of the first hot flame to the upstream side observed in the experiments was well reproduced by the computations.

Table 6.2
Comparisons of wall temperatures at each flame under given conditions in unit K (U = 2.0 cm/sec, d = 1.0 mm, P = 5.0 atm, φ = 1.0).

	Fuel	PRF0	PRF50	PRF100
Experiment	cool flame	683	685	-
	1st hot flame	901	918	975
	2nd hot flame	1146	1147	1138
Computation	cool flame	637	650	688
	1st hot flame	836	889	900
	2nd hot flame	1157	1127	1129

Focusing on the HRR peak value of each flame, the reason why cool flame of PRF100/air was not observed even under the elevated pressure was explained by the computed HRR profile in Fig. 6.14. Although the HRR peak of cool flame increases under elevated pressure, it is much smaller than those in the cases of PRF0/air and PRF50/air. On the other hand, it was not confirmed that the HRR distribution of each flame, that is, cool and first hot flames increase their HRR significantly under the elevated pressure and that the second hot flame becomes even lower than them. It should be noted that since the luminosity profile of flames observed in the experiment and the computed HRR profile are being compared, it is difficult to discuss the quantitative correlation between them.

As shown in Fig. 6.17, computational results show that the difference of the second hot flame position between PRF0 and PRF100 decreases with increasing pressure. Thus, what play a significant role under high pressure are the increasing HRR and the position changes of the cool and the first hot flames to the low temperature region, rather than the position changes of the second hot flame. The same tendency can be expected in the compression ignition-type internal combustion engines which are normally operated under high pressure conditions.

By investigating oxidation characteristics in each temperature region separately for various octane number fuels under elevated pressure, the potential of the micro flow reactor to obtain unique insight into the general ignition characteristics of practical fuels was confirmed. Further investigation may possibly show an alternative index to the octane number which systematizes ignition characteristics of practical fuels. Regarding that point, the capability of the micro flow reactor with a controlled temperature profile to separate the oxidation process into each temperature range is expected to be of practical use for future alternative fuel characterization.

In this study, only stoichiometric mixture was used just for obtaining basic knowledge on overall behavior of the flames. The effect of equivalence ratio will be examined in the future.

6.4. Conclusions

Combustion and ignition characteristics of PRF/air mixtures were investigated using a micro flow reactor with a controlled temperature profile.

Flame responses to various inlet flow velocities were examined using PRF100 (iso-octane 100%) as a fuel since PRF0 (n-heptane) case was already addressed in our previous study [17]. Three different flame patterns were observed: normal propagating flame in a high flow velocity region; FREI in an intermediate flow velocity region; and stable weak flames in a low flow velocity region. This tendency agreed with the previous studies using other fuels.

By focusing on weak flames in the low flow velocity region, weak flame responses to fuels with various RONs were examined by changing the mixing ratio of iso-octane and n-heptane. The cool flame was weakened, and second hot flame shifted to the higher

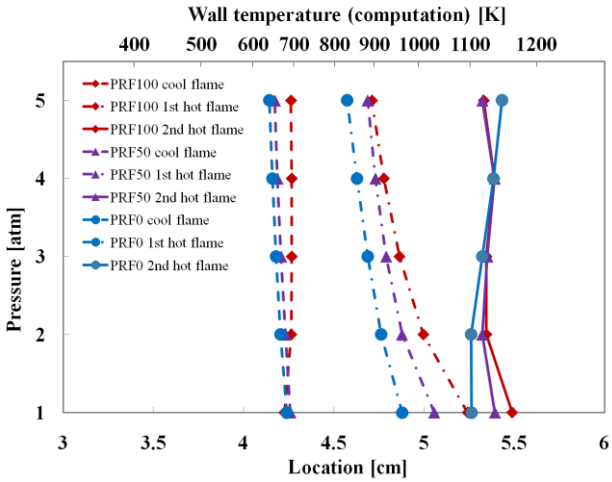

Fig. 6.17. Experimentally confirmed weak flame position to pressure.

temperature region as RON increased. To examine the experimental results, 1-D computations were conducted to investigate the weak flame responses to various RONs. Computed HRR profiles successfully reproduced the experimental results. By conducting the experiments and computations to investigate the weak flame responses to RONs, the capability of the micro flow reactor to distinguish and examine the different ignition process for fuels with different octane number was demonstrated.

In addition, experiment and computation were conducted to investigate the response of weak flames to elevated pressures. It was confirmed that as the pressure increased, cool and first hot flame increased their luminosities and shifted to the low temperature region. These tendencies were intensified, especially for the low octane-rated PRF. As a result, it was found that the difference of ignition characteristics of fuels with different octane numbers is characterized by low and intermediate temperature oxidation, especially under elevated pressure.

Results of this study confirmed the possibility of using the micro flow reactor with a controlled temperature profile to investigate the ignition characteristics of practical fuels. The advantage of the investigation of the oxidation process in each temperature region was indicated for a detailed understanding of the ignition phenomena. The obtained results should be useful in various ways, for example, in reaction path analysis, and in the development and validation of reaction kinetics.

References

[1]R. Minetti, M. Carlier, M. Ribaucour, E. Therssen, L.R. Sochet, Combust. Flame 102 (3) (1995) 298‑309.

[2]D. Healy, H.J. Curran, J.M. Simmie, D.M. Kalitan, C.M. Zinner, A.B. Barrett, E.L. Petersen, G. Bourque, Combust. Flame 155 (2008) 441‑448.

[3]S. Tanaka, F. Ayala, J.C. Keck, J.B. Heywood, Combust. Flame 132 (1‑2) (2003) 219‑239.

[4]J.F. Griffiths, P.A. Halford-Maw, D.J. Rose, Combust. Flame 95 (1993) 291‑306.

[5]K. Maruta, T. Kataoka, N.I. Kim, S. Minaev, R. Fursenko, Proc. Combust. Inst. 30 (2005) 2429‑2436.

[6]K. Maruta, J.K. Parc, K.C. Oh, T. Fujimori, S.S. Minaev, R.V. Fursenko, Combust. Explos. Shock Waves 40 (5) (2004) 516 ‑523.

[7]A.C. Fernandez-Pello, Proc. Combust. Inst. 29 (2002) 883‑899.

[8]P.D. Ronney, Combust. Flame 135 (4) (2003) 421‑439.

[9]Yiguang Ju, Kaoru Maruta, Prog. Energy Combust. Sci. 37(6) (2011) 669-715.

[10]F. Richecoeur, D.C. Kyritsis, Proc. Combust. Inst. 30 (2005) 2419‑2427.

[11]D.G. Norton, D.G. Vlachos, Chem. Eng. Sci. 58 (2003) 4871–4882.

[12]Y. Fan, Y. Suzuki, N. Kasagi, Proc. Combust. Inst. 32 (2009) 3083‑3090.

[13]G. Pizza, C.E. Frouzakis, J. Mantzaras, A.G. Tomboulides, K. Boulouchos, Combust. Flame 155 (2008) 2‑20.

[14]Y. Tsuboi, T. Yokomori, K. Maruta, Combust. Sci. Technol. 180 (10) (2008) 2029‑2045.

[15]Y. Tsuboi, T. Yokomori, K. Maruta, Proc. Combust. Inst. 32 (2009) 3075‑3081.

[16]H. Oshibe, H. Nakamura, T. Tezuka, S. Hasegawa, K. Maruta, Combust. Flame 157 (8) (2010) 1572‑1580.

[17]A. Yamamoto, H. Oshibe, H. Nakamura, T. Tezuka, S. Hasegawa, K. Maruta, Proc. Combust. Inst. 33 (2) (2011) 3259-3266.

[18]Curran, H. J., P. Gaffuri, W. J. Pitz, C. K. Westbrook, Combust. Flame 129 (2002) 253-280.

[19]Curran, H. J., W. J. Pitz, C. K. Westbrook, C. V. Callahan, F. L. Dryer, Proc. Combust. Inst. 27 (1998) 379-387.

[20]R.J. Kee, J.F. Grcar, M.D. Smooke, J.A. Miller, A Fortran Program for Modeling Steady Laminar One-dimensional Premixed Flames, Report No. SAND85-8240, Sandia National Laboratories, 1985.

[21]S. Minaev, K. Maruta, R. Fursenko, Combust. Theor. Model. 11 (2) (2007) 187‑203.

[22]C.J. Evans, D.C. Kyritsis, Proc. Combust. Inst. 32 (2009) 3107‑3114.

[23]C.K. Westbrook, Proc. Combust. Inst. 28 (2) (2000)1563–1575.

[24]H. Yamada, K. Suzaki, A. Tezaki, Y. Goto,Combust. Flame 154 (1–2) (2008) 248–258.

[25]R.S. Sheinson, F.W. Williams, Combust. Flame 21(2) (1973) 221–230.

[26]S. Sueyasu, T. Hikita, Combust. Flame 9 (1) (1965)1–6.

[27]Z. Zheng, M. Yao, Fuel 85 (17–18) (2006) 2605–2615.

[28]I. Glassman, Combustion, fourth ed., AcademicPress, 2008, pp. 117.